

	SAKARYA ÜNİVERSİTESİ FEN BİLİMLERİ ENSTİTÜSÜ DERGİSİ SAKARYA UNIVERSITY JOURNAL OF SCIENCE		
	e-ISSN: 2147-835X Dergi sayfası: http://www.saujs.sakarya.edu.tr		
	Geliş/Received 08-02-2017 Kabul/Accepted 31-10-2017	Doi 10.16984/saufenbilder.290819	

Analysis of ejector expansion refrigeration cycle with two phase flow ejector

Candeniz Seçkin*¹

ABSTRACT

The aim of this study is to determine the operational characteristics of an ejector expansion refrigeration cycle (EERC) working with refrigerant R134a. A constant-area two phase flow ejector at critical mode is modeled to determine the effect of condenser pressure (P_{cond}) and evaporator pressure (P_{evap}) on the performance parameters of EERC: ejector expansion factor (EEF) and coefficient of performance (COP). Additionally, since it is possible to use the EERC for different cooling requirements, variation of COP and EEF with Q_{evap} is also investigated. For this purpose, a simulation program is developed using EES software. The two-phase/compressible fluid flow in the ejector is analyzed accounting for real gas behavior of the refrigerant. Extensive details of mathematical modeling and applied computational procedure are also presented in the study.

Anahtar Kelimeler: Ejector, Ejector expansion refrigeration cycle, Constant-area ejector

İki fazlı ejektör kullanan ejektörlü soğutma çevriminin analizi

ÖZ

Bu çalışmanın amacı, R134a soğutucu akışkan ile çalışan bir ejektör genişleme soğutma çevriminin (EERC) çalışma karakteristiklerinin belirlenmesidir. Kritik modda çalışan, iki fazlı ve sabit alanlı bir ejektör, yoğunlaştırıcı basıncı (P_{cond}) ve buharlaştırıcı basıncının (P_{evap}), ejektör genişleme faktörü (EEF) ve performans katsayısı (COP) üzerindeki etkilerinin belirlenmesi için modellenmiştir. EERC'nin farklı soğutma yükü ihtiyaçlarında kullanılması mümkün olduğundan, COP ve EEF'nin soğutma kapasitesi (Q_{evap})'ne bağlı değişimleri de incelenmiştir. Bu amaçla, EES programı kullanılarak bir simülasyon programı geliştirilmiştir. Ejektör içindeki iki fazlı/sıkıştırılabilir akış modellenirken soğutucunun gerçek gaz davranışı hesaba katılmıştır. Geliştirilen matematiksel model ve hesaplama prosedürü detayları ile sunulmuştur.

Keywords: Ejektör, Ejektörlü soğutma çevrimi, Sabit-alanlı ejektör

¹ Department of Mechanical Engineering, Faculty of Engineering, Marmara University, Goztepe Campus, Istanbul 34722, Turkey
 candeniz.seckin@marmara.edu.tr

1. INTRODUCTION

In classical vapor compression refrigeration cycle (VCRC, reversed Rankine cycle), one of the major reason of efficiency loss is the throttling loss in the expansion valve which is originated by the isenthalpic expansion of the refrigerant from the condensation pressure to the evaporation pressure of the cycle. One of the efficient ways of improving the efficiency is replacing the isenthalpic expansion valve of the classical refrigeration cycle by a device that operates closer to ideal isentropic expansion process. When an ejector is used as a substitute of the expansion valve in the refrigeration cycle, the expansion work lost during isenthalpic expansion process is recovered which means higher ejector outlet pressure, i.e., higher pressure at the compressor inlet. Hence, use of ejector in the refrigeration cycle reduces the power requirement of the compressor, and additionally, supplying the higher pressure refrigerant to the compressor also effectively increases the capacity of the cycle. As a result, replacement of expansion valve by an ejector is a reasonable and effective modification in refrigeration technology to reduce the energy consumption of the total refrigeration cycle and hence, to increase the efficiency of the cycle [1-3].

As a result of the above mentioned advantages, ejector expansion refrigeration cycles (EERC) have recently received considerable attention. The preliminary efforts of modeling EERC cycles are performed for single-phase working fluids. While most of the studies are performed for transcritical applications of high pressure fluids, i.e. carbon dioxide, later thermodynamic analyses showed that ejectors offer remarkable efficiency improvement in refrigeration systems working with low pressure refrigerants, as well. At low pressures (in subcritical region) the phase of the substance is saturated mixture while passing through the ejector and “two phase flow ejector” name is employed to emphasize the existence of two phase refrigerant in the ejector. A two-phase ejector performs expansion, mixing and compression of the refrigerant fluxes consecutively [1, 2]. However, approaches applied in mathematical modeling of a two-phase flow ejector to determine the design parameters and the operational conditions are significantly different than those of a single-phase flow application [4]. In this study, a detailed theoretical investigation of

using a two-phase flow ejector expansion device in a refrigeration cycle is presented.

In supersonic ejector applications, one of the most important operational parameters which has a significant effect on ejector performance is the entrainment ratio (w). The physical meaning of w is ratio of mass flow rate of two streams (motive stream and secondary stream) in the ejector and detailed explanation is available in further sections of this study. To describe the ejector performance in terms of entrainment ratio, operational modes of the ejector can be divided into three modes: critical mode, sub-critical mode and back pressure mode [5-9]. Variation of entrainment ratio with back pressure of the ejector is shown in Fig. 1 when inlet pressure of the streams is constant. During critical mode operation, the motive and the secondary flows are both choked, and the entrainment ratio (w) reaches a maximum value that remains constant. When the operation mode is the critical mode, back pressure of the ejector is low. At sub-critical mode of operation, only the motive flow is choked and the entrainment ratio is not constant but varies with the back pressure. At the back flow mode, the secondary flow is reversed and the entrainment ratio is less than zero. Munday and Bagster [9] reported the results of a secondary flow choking in the converging nozzle before mixing with the motive steam. The supersonic mixture with uniform pressure that obtained is compressed by a shock wave in the constant area mixing section before discharging to the outside of the diffuser. The ejector is supposed to operate at critical mode and refrigeration performance is determined to be optimal at critical mode. Eames et al. [10] reported their experimental and theoretical study of ejector refrigeration system. The maximum COP was obtained when the ejector was operated at critical mode. Huang et al. [5] proposed a 1-dimensional modeling procedure for a constant pressure ejector operating at critical mode with ideal gas assumption. It is obtained that the system reaches its maximum performance at critical mode. In this study, considered ejector in EERC is analysed at critical mode of operation.

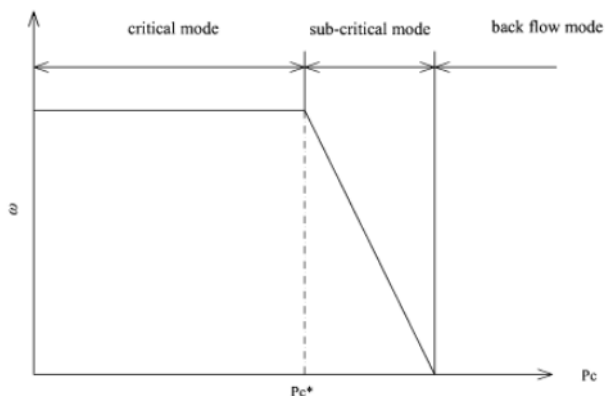


Figure 1. Operational modes of ejector

The first attempt of the two-phase ejector cycle application was performed by Gay [11]. This cycle has received the majority of the attention in two-phase ejector studies. Kemper et al. [12], Newton [13] and Newton [14] modified the Gay's cycle to have better cooling performance. One of the first theoretical analysis of EERC is performed by Kornhauser [15] and a 1-D, homogeneous equilibrium model with the assumption of constant pressure mixing for two-phase ejector is developed. The proposed model is broadly accepted and has been used extensively in theoretical works analysing two-phase ejectors. The ejector is two-phase and COP is determined for different refrigerants. Theoretical COP increase of 13, 21, 20, and 12 % is reported for refrigerants of R11, R12, R22 and ammonia, respectively, relative to classical VCRC. Domanski [16] investigated the performance of 38 different refrigerants by utilizing the model by Kornhauser [15] in a two-phase EERC. R218 is determined as the highest COP providing refrigerant with almost 60 % COP increase over classical VCRC operating under the same conditions. In this study, COP improvement of R12, R22, R32, R134a, propane, isobutane, and ammonia is found to be between 10 - 30 % theoretically. Nehdi et al. [17] reported that COP of the cooling cycle is possible to be improved by 22% with R141b and 20 % with R410A in a two-phase ejector EERC compared to VCRC. Experimental results for two phase ejector refrigeration cycle using R134a refrigerant are reported by Harrell and Kornhauser [18]. Another experimental study of two phase ejector cycle is performed by Nakagawa et al. [19] with the refrigerant of R12. They found that longer mixing section, lower entrainment ratio and smaller mixing diameter give higher results of ejector pressure lift (the ratio of pressure at the diffuser exit to that of the secondary nozzle inlet). Nakagawa and Tackeuchi [20] showed the results

of ejectors with different geometries and all working with R134a. It is stated that better ejector performance is provided when primary nozzle diverging length is longer. COP improvement of 10 % over a classical VCRC is determined for a standard two-phase ejector cycle. Experimental works which compare a two-phase EERC to a classical VCRC are conducted by Disawas and Wongwises [21] and Wongwises and Disawas [22] with refrigerant of R134a. COP improvements of about 5 % are reached. The effect of primary nozzle throat diameter on the cooling performance and efficiency of EERC with two-phase ejector is analysed experimentally by Chaiwongsa and Wongwises [23]. The cycle operates with R134a. It is found that the smaller the primary nozzle throat diameter is, the higher the cooling capacity and COP are. Chaiwongsa and Wongwises [24] experimentally determined that variation in primary nozzle outlet diameter does not result in considerable change in COP of the EERC. Khalil et al. [25] developed a mathematical model to design a constant pressure ejector and the remaining refrigeration cycle working with R134a. Seckin [26] performed a similar analysis for a ejector refrigeration cycle with a constant pressure ejector. Tashtoush et al. [27] selected ejector refrigeration cycle with refrigerant R134a as the basic cycle and investigated the performance of other refrigerants only at critical mode. Experimental results of refrigeration cycle with constant area ejector using R-134a refrigerant are also presented by Ersoy and Bilir Sag [28], Bilir Sag et al. [29] and Yapici et al. [30].

In this present study, effect of condenser pressure and evaporator pressure on the performance parameters of EERC: ejector expansion factor (EEF) and coefficient of performance (COP). Additionally, since it is possible to use the EERC for different cooling requirements, variation of COP and EEF with cooling capacity is also investigated. The analysis is performed for a constant-area type ejector. The ejector operates at critical mode, i.e. the primary and secondary flows are both choked and the entrainment is constant [25]. The considered EERC is modeled by using EES software (Engineering Equation Solver). The real gas thermodynamic properties of R134a are used to have more accurate results which are away from the analytical deviation occurs when ideal gas assumption is applied [31-33]. Normal shock takes place at the end of the constant area mixing chamber [25, 34, 35]. Modeling procedure has some common points with that of [25] but in this

present study, 1) the type of the ejector is constant-area ejector (not constant-pressure as it is in [25]) 2) design of the analysed ejector refrigeration cycle (EERC) is different and 3) thermodynamic properties of the fluid at critical conditions are determined by Henry and Fauske method (i.e. an iterative computational procedure conducted based on determining the maximum flow rate is not applied). The modeling procedure and design conditions in this study are also different from [34] and [35]. Extensive discussion of computational details and Henry and Fauske method is presented in further sections of this study.

2. EJECTOR EXPANSION REFRIGERATION CYCLE AND EJECTOR DESIGN

Schematic of considered EERC is seen in Fig. 2 with corresponding P-h diagram of the cycle. The main components of the EERC are: compressor, evaporator, condenser, ejector and separator. Ejector is the key component of EERC. The difference between EERC and VCRC is extra components of: two-phase flow ejector and separator chamber in the ejector expansion cycle. The refrigerant exits from ejector as saturated mixture and enters the separator. The separator is assumed to be 100% efficient and hence, the refrigerant is split into two parts perfectly: saturated vapor and saturated liquid parts. The saturated vapor refrigerant circulates the upper loop of the EERC (seen in Fig. 2). First, the refrigerant is compressed to a high pressure by the compressor. The phase of the refrigerant is superheated vapor at the compressor exit (state point 5). The superheated vapor refrigerant is condensed in the condenser (heat is discharged from the refrigerant to the surrounding medium through the condenser, Q_{cond}). At the exit of the condenser (at the inlet of the ejector primary nozzle, state point 1 in Fig. 2) the phase of the refrigerant is saturated liquid and the pressure is condenser pressure. This flow is named “motive flow” which is sucked by the primary nozzle of the ejector. The saturated liquid part of the refrigerant at the separator exit (state point 6) leaves the separator and circulates the lower loop of the cycle in Fig. 2. The refrigerant is expanded in the expansion device (state point 7). Then the refrigerant is evaporated in the evaporator (heat is extracted from the cooled environment and is transferred to the refrigerant while passing through the evaporator, Q_{evap}). At the exit of the evaporator

(at the inlet of the ejector secondary nozzle, state point 2 in Fig. 2), the phase of the refrigerant is saturated vapor and the pressure is evaporator pressure. This flow is named “secondary flow” which is sucked by the secondary nozzle of the ejector [36].

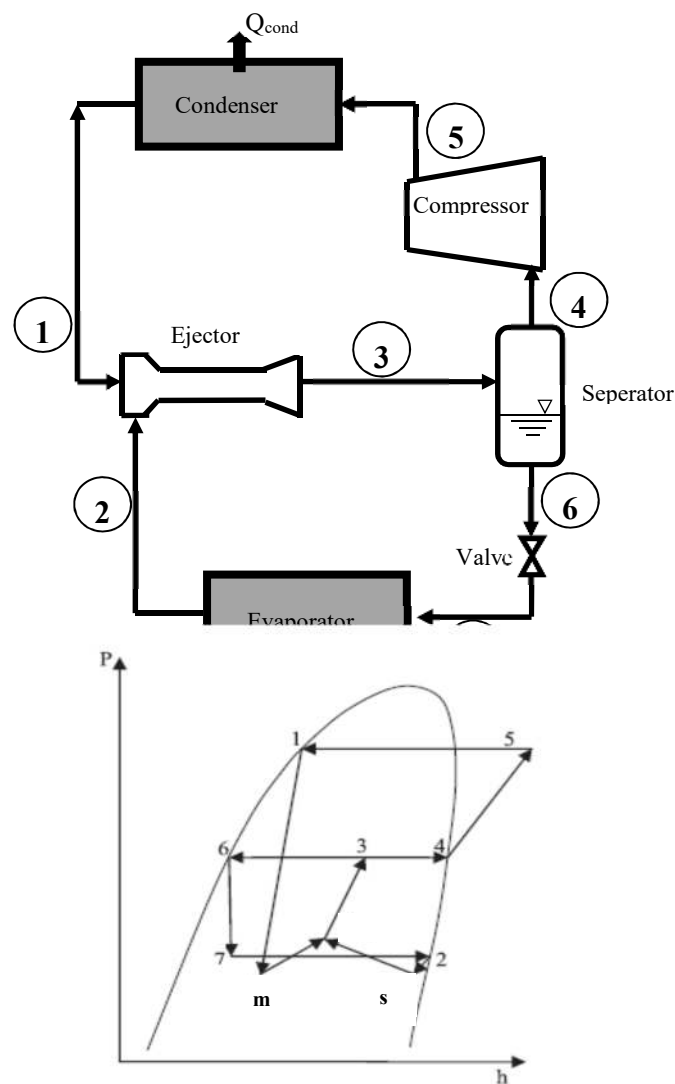


Figure 2. a) Schematic overview of EERC b) P-h diagram of EERC.

In a refrigeration cycle, the function of an integrated two-phase ejector is twofold: expansion of the primary stream fed from the condenser, and compression of the secondary stream drawn from the evaporator. Ejector is essentially composed of a primary nozzle (converging- diverging nozzle), secondary nozzle (converging only), constant area mixing section and diffuser (Fig. 3). Mostly encountered ejector designs can be categorized into two types based on the location of primary and secondary nozzle exits: “constant area ejector” and “constant pressure ejector”. In constant area type ejector design, the primary and secondary nozzle

exits are located at the beginning of the “constant area mixing chamber” of the ejector (Fig. 3). In the other type of the ejector, exits of the nozzles are located prior to the beginning of “constant area mixing chamber”. In both designs, the mixing process takes place inside the constant area mixing chamber [5, 36]. In this study, a constant area ejector is analyzed and mathematical modeling of the ejector is presented in details in the further sections.

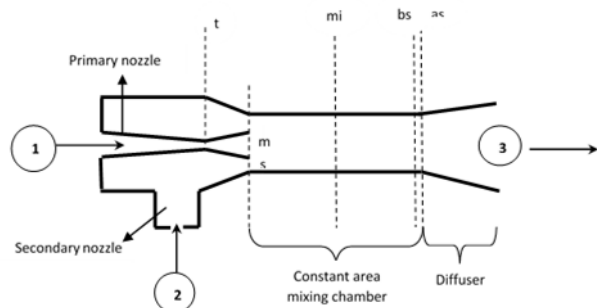


Figure 3. Constant area ejector design

Operational principle of constant area ejector is illustrated in Fig. 3. The high-pressure motive flow (state point 1) is expanded in the converging-diverging primary nozzle to the pressure P_m (at cross section m in Fig. 3) which is lower than the evaporator pressure (P_{evap}). Due to the vacuum effect, which occurs at the exit of the primary nozzle for the secondary flow, the secondary flow is sucked into the ejector. The secondary flow is to be expanded through the secondary nozzle to the pressure P_s (at cross section s in Fig. 3) and then, both refrigerant streams are mixed in the “constant area mixing chamber” at constant pressure (cross section “mix” in Fig. 3). A normal shock wave takes place in the constant-area mixing chamber (specifically at the end of the constant area mixing chamber in this study, cross section “bs” in Fig. 3) and hence, velocity of the refrigerant decreases and the pressure increases where the normal shock occurs (at the cross section “as” in Fig. 3). In the diffuser, the pressure of the refrigerant increases further and the phase of the refrigerant is saturated mixture at the ejector exit (state point 3). An intermediate pressure is reached at the exit of the ejector (P_3) which is between the motive and secondary stream pressures (P_1 and P_2) and is equal to separator pressure [35, 37].

3. MATHEMATICAL MODELING AND COMPUTATIONAL ANALYSIS

As it is stated above, the performance of the ejector is crucial for the performance of EERC since the

ejector recovers the expansion process losses and increases the inlet pressure of the compressor, i.e., the use of ejector in EERC increases the refrigeration system overall efficiency by reducing the power requirement of the compressor. As a result, understanding the operational mechanism of the ejector and modeling the ejector properly have the corresponding importance. Applied assumptions in mathematical modeling of the system are listed below [34, 38, 39]:

1. One-dimensional and steady state flow through the ejector.
2. Primary and secondary fluids are supplied at zero velocities (stagnation conditions) at state points (1) and (2). Also, velocity of compressed mixture at the exit of diffuser (state point 3 in Fig 2) is zero (stagnation condition).
3. Pressure is constant in the mixing process.
4. Friction losses are defined in terms of isentropic efficiencies in the nozzles and diffuser.
5. The design pressure at the primary nozzle exit is uniform (cross section “m” in Fig 3) and the secondary stream velocity reaches the speed of sound at this level (cross section “s” in Fig 3).
6. Critical-mode operation, i.e. the primary and secondary flows are both choked and the entrainment is constant.
7. Normal shock occurs at the end of the constant area mixing chamber.
8. The heat transfer between the fluid and ejector wall is neglected.
9. The gravitational force effect on the flow is neglected.
10. Within the condenser and evaporator, pressure and temperature are constant.

The mathematical representation of refrigerant flow inside the ejector and also in different components of EERC is complex. Additional complexity occurs when two-phases are present in the flow. In this study, to determine the critical properties of the two-phase flow, Henry and Fauske method [40] is applied and details are given in the following sections. It should be noticed that Henry and Fauske [40] used experimental data of refrigerant R744 to validate their model and this renders the model credible. In order to eliminate the analytical error induced by the ideal gas assumption when the ejector issued with refrigerants, the thermodynamics properties of real gases were used [31, 32, 33] to apply mass,

momentum, and energy conservation principles. Below, governing equations are derived by applying the conservation of mass, energy and momentum principles to each part of the ejector to determine the main dimensions and performance characteristics of EERC. Added to this, thermodynamic analysis of the other components of the EERC is also presented.

3.1. Primary Nozzle

Specific enthalpy of the motive stream at the primary nozzle exit (h_m) is calculated as follows based on the isentropic efficiency of nozzle:

$$h_m = h_1 (1 - \eta_p) + \eta_p h_{m,is} \quad (1)$$

$$h_{m,is} = f(P_m, s_1) \quad (2)$$

where η_p is the primary nozzle isentropic efficiency, $h_{p,is}$ is the specific enthalpy of the motive stream at the end of the isentropic expansion process in the primary nozzle, h_1 is the specific enthalpy of the motive stream at the nozzle inlet, P_m is the motive stream pressure at the primary nozzle exit, s_1 is the specific entropy of the motive stream at the nozzle inlet.

Applying the conservation of energy principle between primary nozzle inlet and outlet, following equation is obtained, where V_m is the velocity of the motive stream at the primary nozzle exit:

$$V_m = \sqrt{2(h_1 - h_m)} \quad (3)$$

Based on the conservation of mass equation, the following equation is obtained for the primary nozzle:

$$m_1 = \left(\frac{1}{1+w} \right) m_{tot} = \frac{V_m A_m}{v_m} \quad (4)$$

$$v_m = f(P_m, h_m) \quad (5)$$

where w is the entrainment ratio which is the ratio of the secondary stream mass flow rate (m_2) to the motive stream mass flow rate (m_1), m_{tot} is the total mass flow rate of the refrigerant (m_1+m_2), A_m and v_m are the cross-sectional area and the specific volume at the primary nozzle exit, respectively.

3.2. Secondary Nozzle

In a real ejector, the secondary nozzle is a chamber through which secondary stream is transferred to constant area mixing chamber due to the pressure difference at the exit. However, in ejector modeling studies (presented earlier), the secondary

stream is modeled in such a manner so that expansion of the secondary flow occurs in a converging nozzle (which is called secondary nozzle) [39].

At the nozzle outlet (cross-section m and s), the motive stream pressure becomes lower than secondary stream pressure and secondary stream is transferred to the constant area mixing section by means of the pressure difference between primary and secondary streams pressures (P_m and P_s). It is assumed that the secondary fluid leaves the secondary nozzle at critical pressure, i.e., $Ma_s = 1$ [25, 38]. Critical properties of the secondary stream are determined by applying Henry and Fauske method. Details of the method are presented further.

Specific enthalpy of the secondary stream at the secondary nozzle exit (h_s) is calculated as follows based on the isentropic efficiency of nozzle:

$$h_s = h_2 (1 - \eta_s) + \eta_s h_{s,is} \quad (6)$$

$$h_{s,is} = f(P_s, s_2) \quad (7)$$

where η_s is the secondary nozzle isentropic efficiency, $h_{s,is}$ is the specific enthalpy of the secondary stream at the end of the isentropic expansion process in the secondary nozzle, h_2 is the specific enthalpy of the secondary stream at the nozzle inlet, P_s is the secondary stream pressure at the secondary nozzle exit, s_2 is the specific entropy of the secondary stream at the nozzle inlet.

Applying the conservation of energy principle between secondary nozzle inlet and outlet, following equation is obtained, where V_s is the velocity of the secondary stream at the secondary nozzle exit:

$$V_s = \sqrt{2(h_2 - h_s)} \quad (8)$$

Based on the conservation of mass equation, the following equation is obtained for the secondary nozzle:

$$m_2 = \left(\frac{w}{1+w} \right) m_{tot} = \frac{V_s A_s}{v_s} \quad (9)$$

$$v_s = f(P_s, h_s) \quad (10)$$

$$x_s = f(P_s, h_s) \quad (11)$$

where x_s is the quality of secondary stream at nozzle exit, A_s and v_s are the cross-sectional area and the specific volume at the secondary nozzle exit, respectively.

3.3. Constant Area Mixing Chamber

The constant area mixing chamber starts from the exits of the primary nozzle and the secondary nozzle to the inlet of diffuser section (between cross-section “m+s” and “as” in Figure 3). To model and simulate the constant area mixing chamber, below listed assumptions are applied:

- At the inlet plane (m), the motive stream has the velocity of V_m , pressure of P_m , and occupies the cross-sectional area A_m .
- At the inlet plane (s), the secondary stream has the velocity of V_s , pressure of P_s , and occupies the cross-sectional area A_s .
- At the cross section (mix), the flow becomes uniform and has the velocity of V_{mix} and pressure of P_{mix} .
- A constant pressure mixing process occurs between the motive stream and secondary stream (between cross-sections (m+s) – (mix) in Fig. 3).
- Normal shock occurs at the exit of the constant area mixing chamber. The cross sectional area is A_{bs} just before the shock and A_{as} after the shock.

$$A_{bs} = A_{as} = A_s + A_m \quad (12)$$

Conservation of mass, momentum and energy equations for the flow “before shock” (at the cross-section “bs” in Fig. 3) are developed and presented between Eq. (13)-(15):

$$m_{tot} = \frac{V_{bs} A_{bs}}{v_{bs}} \quad (13)$$

where V_{bs} and v_{bs} are velocity and specific volume of the refrigerant at cross-section “bs” in Fig. 3, respectively.

Conservation of momentum equation:

$$P_{bs} A_{bs} + m_{tot} V_{bs} = \phi_m (P_m A_m + m_1 V_m + P_s A_s + m_2 V_s) = \left(P_m A_m + \frac{A_m V_m^2}{v_m} + P_s A_s + \frac{A_s V_s^2}{v_s} \right) \quad (14)$$

where P_{bs} is the pressure of the mixed flow at the end of the constant area mixing section (before shock), ϕ_m is the coefficient accounting for the frictional loss [5, 41].

Under the assumption of P_{bs} is known, inserting A_{bs} and m_{tot} into the Eq. (14), V_{bs} is possible to be determined. Using V_{bs} in Eq. 13, v_{bs} is also obtainable.

Conservation of energy equation:

$$m_{tot} \left[h_{bs} + \frac{V_{bs}^2}{2} \right] = m_1 \left[h_m + \frac{V_m^2}{2} \right] + m_2 \left[h_s + \frac{V_s^2}{2} \right] \quad (15)$$

Inserting V_{bs} into Eq. (15), h_{bs} (specific entropy of the refrigerant before shock) can be determined. Then,

$$P_{bs} = f(h_{bs}, v_{bs}) \quad (16)$$

$$x_{bs} = f(P_{bs}, h_{bs}) \quad (17)$$

Determined v_{bs} and h_{bs} must comply with the thermodynamic relation presented in Eq. (16). In Eq. (17), x_{bs} is the quality of the refrigerant if exists.

The ejector is designed in such a manner so that normal shock takes place at the end of constant area mixing chamber, i.e., $Ma=1$ at the cross-section “bs” in Fig. 3. If the phase of the substance is saturated mixture, Henry and Fauske method is applied to determine the fluid properties before shock. If the phase is superheated vapor, below procedure is applied:

$$Ma=1 = \frac{V_{bs}}{C_{bs}} \quad (18)$$

$$C_{bs} = f(P_{bs}, h_{bs}) \quad (19)$$

where C_{bs} is the speed of sound at cross-section “bs” (before shock). Pressure of the mixed refrigerant before the shock wave occurs (P_{bs}) is iterated until Mach number at the mixed section reaches unity (Eq. (18)).

In Fig. 3, cross-section “as” represents the flow after the shock occurs. Equations of mass, momentum and energy conservation principles as well as entropy balance before and after the normal shock are applied in below equations between cross-sections “bs” and “as” [42]. In the equations, A_{as} , P_{as} , V_{as} , v_{as} , h_{as} and s_{as} are area, pressure, velocity, specific volume, specific enthalpy and specific entropy at the cross-section “as” in Fig. 3, respectively.

$$A_{bs} = A_{as} \quad (20)$$

Conservation of mass equation:

$$m_{bs} = m_{as} \Rightarrow \frac{A_{bs} V_{bs}}{v_{bs}} = \frac{A_{as} V_{as}}{v_{as}} \Rightarrow v_{as} = \frac{V_{as} v_{bs}}{V_{bs}} \quad (21)$$

Conservation of momentum equation:

$$P_{bs} A_{bs} + m_{tot} V_{bs} = P_{as} A_{as} + m_{tot} V_{as}$$

$$\Rightarrow V_{as} = \frac{(P_{bs} - P_{as}) A_{as}}{m_{tot}} + V_{bs} \quad (22)$$

Conservation of energy equation:

$$h_{bs} + \frac{V_{bs}^2}{2} = h_{as} + \frac{V_{as}^2}{2} \quad (23)$$

$$P_{as} = f(v_{as}, h_{as}) \quad (24)$$

$$s_{as} = f(P_{as}, h_{as}) \quad (25)$$

$$s_{as} > s_{bs} \quad (26)$$

3.4. Diffuser

Specific enthalpy at the diffuser exit (h_3) can be obtained by applying conservation of energy equation:

$$m_{tot} h_3 = m_1 h_1 + m_2 h_2 \quad (27)$$

Another way to determine h_3 is to be introduced by using diffuser isentropic efficiency (η_d) as presented below:

$$\eta_d = \frac{h_{3,is} - h_{as}}{h_3 - h_{as}} \quad (28)$$

$$h_{3,is} = f(P_3, s_{as}) \quad (29)$$

where $h_{3,is}$ is the specific enthalpy at the end of an isentropic process in the diffuser, P_3 is the pressure at the exit of the diffuser and s_{as} is the specific entropy at the diffuser inlet (after shock).

The diffuser outlet quality (x_3) is obtained from thermodynamic property relation:

$$x_3 = f(P_3, h_3) \quad (30)$$

In Eq. (31), the relation between the entrainment ratio (w) and the quality of the refrigerant at the ejector outlet (x_3) is presented. To realize the considered refrigeration cycle, Eq. (31) must be satisfied.

$$x_d (1 + w) = 1 \quad (31)$$

3.5. Determination of Critical Flow Properties - Henry and Fauske Method

As stated in earlier sections, in this present study, a constant area ejector is analysed under the critical operation mode conditions, i.e., the primary and secondary flows are both choked and the entrainment is constant. Considered ejector is a two phase flow ejector, hence, at the cross

section “t” in the motive nozzle and at the cross section “s” in the secondary nozzle (Fig. 3), the flows are two-phase critical flows. In this study, diameters of the ejector and thermodynamic properties of two-phase refrigerant at critical conditions are determined by using empirical flow model proposed by Henry and Fauske [40]. Henry and Fauske [40] made credible assumptions to mathematically express the critical pressure ratio as a function of the input pressure and quality of the refrigerant. It must be underlined that the model is validated by experiments performed with R744 refrigerator in [40] and this is the substantial reason to use their model in this study. The obtained results from the model showed good agreement with the experimental data. In the literature, Henry- Fauske model is used in different studies [21, 22, 24, 43- 46].

The formulas introduced by Henry and Fauske (1971) [40] to determine the critical mass flux (G_c , mass flow rate per unit cross-sectional area at critical cross section) are presented below, in Eq. (33) and (34). G_c is to be calculated by simultaneous solving of below equations [40]. Mathematical definition of G_c is presented in Eq. (32):

$$G_c = \frac{m}{A} \quad (32)$$

$$G_c^2 = \left[\frac{x_0 v_{g,t}}{n P_t} + (v_{g,t} - v_{f,0}) \left\{ \frac{(1-x_0)N}{s_{g,t} - s_{f,t}} \frac{ds_{f,t}}{dP_t} - \frac{x_0 c_{g,t,p} (1/n - 1/\gamma)}{P_t (s_{g,0} - s_{f,0})} \right\} \right]^{-1} \quad (33)$$

$$(1-x_0) v_{f,0} (P_0 - P_t) + \frac{x_0 \gamma}{\gamma - 1} (P_0 v_{g,0} - P_t v_{g,t}) = \frac{[(1-x_0) v_{f,0} + x_0 v_{g,t}]^2}{2} G_c^2 \quad (34)$$

where x_0 is the quality at the inlet of the flux, P_t is the throat pressure, P_0 is the inlet pressure, $v_{g,t}$ is the specific volume of saturated vapour at the throat pressure, $v_{g,0}$ is the specific volume of saturated vapour at the inlet pressure, $v_{f,0}$ is the specific volume of saturated liquid at the inlet pressure, $s_{f,t}$ is the specific entropy of saturated liquid at the throat pressure, $s_{f,0}$ is the specific entropy of saturated liquid at the inlet pressure, $s_{g,t}$ is the specific entropy of saturated vapour at the throat pressure, $s_{g,0}$ is the specific entropy of saturated vapour at the inlet pressure, $c_{g,t,p}$ is the constant pressure specific heat of the saturated vapour at the throat pressure. N is the partial phase change at the throat and is determined experimentally as presented in Eq. (35). n and γ

are coefficients which are presented in Eq. (36) and (37), respectively.

$$N = \left\{ \begin{array}{ll} x_t / 0.14 & 0 < x_t < 0.14 \\ 1 & x_t > 0.14 \end{array} \right\} \quad (35)$$

n [40] and γ [47] are computed based on below equations:

$$n = \frac{(1 - x_t) (c_{f,t,p} / c_{g,t,p}) + 1}{(1 - x_t) (c_{f,t,p} / c_{g,t,p}) + 1 / \gamma} \quad (36)$$

$$\gamma = \frac{c_{0,p}}{c_{0,v}} \quad (37)$$

where x_t is the quality at the throat, $c_{f,t,p}$ and $c_{g,t,p}$ are the constant pressure specific heat of the saturated liquid and saturated vapour at the throat pressure, respectively. $c_{0,p}$ is the constant pressure specific heat of the refrigerant when $x=x_0$ and $P=P_t$. $c_{0,v}$ is the constant volume specific heat of the refrigerant when $x=x_0$ and $P=P_t$.

3.5.1. Primary Nozzle Throat

The input pressure to the primary nozzle (P_0 in Eq. (34)) is the pressure at state point 1 in Fig 3 (P_1 , condenser pressure) and the quality (x_0) is zero since the refrigerant leaves the condenser at saturated liquid state. For the special case of primary nozzle, mathematical equivalents which are inserted into Eq. (33) and (34) are presented between Eq. (38) – (40). Eq. (38)-(40) are substituted into Eq. (34) and Eq. (41) is obtained. $G_{c,m}$ is determined by Eq. (41) where $G_{m,c}$ is the critical mass flow at the primary nozzle throat and $P_{t,m}$ is the motive stream pressure at the primary nozzle throat.

$$x_0 = x_1 = 0 \quad (38)$$

$$P_0 = P_1 \quad (39)$$

$$v_{f,0} = v_1 \quad (40)$$

$$\left[\frac{P_{t,m}}{P_0} \right] = 1 - \frac{v_{f,0} G_{c,m}^2}{2 P_0} \quad (41)$$

Cross sectional area of primary nozzle throat ($A_{t,m}$) can be determined as:

$$G_{c,m} = \frac{m_1}{A_{t,m}} \Rightarrow A_{t,m} = \frac{m_1}{G_{c,m}} \quad (42)$$

Using the definition of primary nozzle's isentropic efficiency (η_p), the specific enthalpy of the primary fluid at the nozzle throat ($h_{t,m}$) is obtained by the following:

$$h_{t,m} = h_1 (1 - \eta_p) + \eta_p h_{t,m, is} \quad (43)$$

$$h_{t,m, is} = f(P_{t,m}, s_1) \quad (44)$$

where η_p is the primary nozzle isentropic efficiency, $h_{t,m, is}$ is the specific enthalpy of the motive stream at the throat of the primary nozzle at the end of an isentropic expansion process, h_1 and s_1 are the specific enthalpy and specific entropy of the motive stream at the nozzle inlet, respectively.

Velocity of the motive stream at the primary nozzle throat ($V_{t,m}$) is determined by Eq. (45) based on conservation of energy principle:

$$V_{t,m} = \sqrt{2 (h_1 - h_{t,m})} \quad (45)$$

According to the conservation of mass principle, it is required that below equations hold true at the throat of the primary nozzle where $v_{t,m}$ is the specific volume of the motive stream at the throat of the nozzle.

$$m_1 = \left(\frac{1}{1 + w} \right) m_{tot} = \frac{V_{t,m} A_{t,m}}{v_{t,m}} \Rightarrow \quad (46)$$

$$v_{t,m} = \frac{V_{t,m} A_{t,m}}{m_1}$$

$$P_{t,m} = f(v_{t,m}, h_{t,m}) \quad (47)$$

3.5.2. Secondary Nozzle Exit

As it is stated above, the secondary stream leaves the secondary nozzle at critical pressure. Application of Henry and Fauske method to the special case of secondary nozzle exit (Fig. 3) is presented below between Eq. (48 - 55) where $G_{s,c}$ is the critical mass flow at the secondary nozzle exit.

For secondary flow, quality of the refrigerant (x_0) and pressure (P_0) at the inlet are equal to the quality and pressure at state point 2 (Fig 3) as mathematically expressed in Eq. (49) and (50).

$$G_{c,s} = \frac{m_2}{A_s} \quad (48)$$

$$x_0 = x_2 = 1 \quad (49)$$

$$P_0 = P_2 \quad (50)$$

Inserting Eq. (35) into Eq. (32) gives:

$$n = \gamma \quad (51)$$

Based on Eq. (35) and Eq. (36), Eq. (28) becomes:

$$G_{c,s}^2 = \left[\frac{v_{g,t}}{n P_t} \right]^{-1} \quad (52)$$

In Eq. (52), P_t is the throat pressure which refers to the secondary nozzle exit pressure (P_s) for considered special case.

In Henry and Fauske method, expansion process is assumed to be isentropic [40]. Inserting Eq. (52) into Eq. (34) and applying isentropic process assumption, Eq. (34) can be written as Eq. (53).

$$[v_{g,t}]_s^{\gamma-1} = [v_{g,0}]_s^{\gamma-1} \left[(\gamma-1) \left(\frac{1}{2} + \frac{1}{\gamma-1} \right) \right] \quad (53)$$

where $[v_{g,0}]_s$ is the specific volume of saturated vapor at the secondary nozzle inlet pressure which is equal to v_2 (Eq. (54)). $[v_{g,t}]_s$ is the specific volume of the saturated vapor at the throat of the secondary nozzle which is the exit of the nozzle.

$$[v_{g,0}]_s = v_2 \quad (54)$$

After determination of $[v_{g,t}]_s$, throat pressure (P_s) is determined by Eq. (55).

$$P_s = f(v = [v_{g,t}]_s, x = 1) \quad (55)$$

After determination of P_s , computation between Eq. (6)-(10) applied to determine A_s .

An alternative way of determining A_s is inserting P_s into Eq. (52) to determine $G_{c,s}$ and substituting $G_{c,s}$ into Eq. (48). The deviation of A_s which is determined by applying the computational procedure between Eq. (48)-(55) and by this alternative way is checked and it is seen that deviation is strongly negligible.

3.6. Separator, Compressor and Evaporator

The saturated mixture refrigerant leaves the ejector, and is split into saturated liquid and saturated vapour parts in the separator. The separator is 100% efficient. Then,

$$h_4 = f(P_3, x_4 = 1) \quad (56)$$

$$h_6 = f(P_3, x_6 = 0) \quad (57)$$

Applying conservation of energy principle to the expansion valve, below equation is obtained:

$$h_6 = h_7 \quad (58)$$

where h_4 , h_6 and h_7 are specific enthalpy of the refrigerant at state point 4, 6 and 7 in Fig 2, respectively. x_4 and x_6 are quality of the refrigerant at the corresponding state points of EERC in Fig. 2.

Cooling capacity of the cycle (the rate of heat removal from the cold space through the evaporator, \dot{Q}_{evap}) is derived by the below equation:

$$\dot{Q}_{\text{evap}} = \dot{m}_2 (h_2 - h_7) \quad (59)$$

Saturated vapour refrigerant exits from the separator and is compressed in the compressor. Isentropic efficiency of the compressor (η_{cp}) can be computed as follows [48]:

$$\eta_{\text{cp}} = 0.874 - 0.0135 \left(\frac{P_5}{P_4} \right) \quad (60)$$

$$P_3 = P_4 = P_6 \quad (61)$$

$$P_5 = P_1 \quad (62)$$

Using the isentropic efficiency of the compressor, the actual enthalpy at the compressor outlet (h_5) can be found by:

$$\eta_{\text{cp}} = \frac{h_{5,\text{is}} - h_4}{h_5 - h_4} \quad (63)$$

$$s_4 = f(P_4, x_4 = 1) \quad (64)$$

$$h_{5,\text{is}} = f(P_5, s_4) \quad (65)$$

$h_{5,\text{is}}$ is the specific enthalpy at the end of the isentropic process in the compressor, P_3 , P_4 and P_5 are pressure at the state points 3, 4 and 5, respectively. s_4 is the specific enthalpy at the point 4 (Fig 2).

Then, power consumption of the compressor (\dot{W}_{cp}) is determined as follows:

$$\dot{W}_{\text{cp}} = \dot{m}_1 (h_5 - h_4) \quad (66)$$

Definition of COP is presented in Eq. (67). As it is seen in the mathematical definition, COP is a direct measure of cooling performance of the refrigeration cycle. The main function of the ejector in the refrigeration cycle is increasing the pressure of the refrigerant as high as possible to supply the high-pressure refrigerant to the compressor and to decrease the power consumption of the cycle. High pressure refrigerant at the compressor inlet (ejector outlet)

is the primary advantage of the EERC over VCRC. Ejector expansion factor (EEF) is a dimensionless parameter which indicates the difference between the pressure at the inlet of the primary nozzle and the pressure at the exit of the ejector (Eq. (68)). EEF is a significant factor depicting the ejector performance. Cooling capacity is a direct measure of the refrigeration function of the cycle and its computation is presented in Eq. (59).

$$\text{COP} = \frac{\dot{Q}_{\text{evap}}}{\dot{W}_{\text{cp}}} \quad (67)$$

$$\text{EEF} = \frac{P_3}{P_1} \quad (68)$$

The simulation of EERC is carried out by writing a computer program in EES (Engineering Equation Solver) to apply the mathematical model presented above. The flow chart of the mathematical 1-D model is shown in Fig. 4. The refrigerant thermodynamic properties, available in the EES data bank, are incorporated into the program. The program runs with a given set of the input values, including: isentropic efficiencies of the nozzles, diffuser isentropic efficiency, total mass flow rate, evaporator and condenser pressures.

4. RESULTS AND DISCUSSION

Considering the cooling system presented in Fig. 2, external parameters which are independent from internal operational characteristics of the refrigeration system (EERC) are: type of the refrigerant, temperature and pressure of the condenser, temperature and pressure of the

evaporator and efficiencies of ejector parts (primary nozzle efficiency, secondary nozzle efficiency and diffuser efficiency). It is also possible to analyze the effect of different system parameters (such as: ejector dimensions, entrainment ratio, etc.) on the performance of the EERC but these system parameters are already a function of above listed external parameters. Thereby, in this present study, a constant-area two phase flow ejector at critical mode is simulated to evaluate the effect of condenser and evaporator pressure on the characteristic performance parameters of: ejector expansion factor (EEF) and coefficient of performance (COP) in the ejector expansion refrigeration system (EERC) working with R134a. Additionally, since it is possible to use the EERC cycle for different cooling requirements, variation of COP and EEF with \dot{Q}_{evap} is investigated.

4.1. Effect of Evaporator Pressure

In Fig. 5, COP and compressor power consumption of the refrigeration cycle (\dot{W}_{cp}) with respect to variation of evaporator pressure (P_{evap}) is seen for constant condenser pressure of 1.8 MPa.

Additionally, variation of EEF and \dot{W}_{cp} of the refrigeration cycle with evaporator pressure (P_{evap}) is reported in Fig. 6. In the analysis, primary nozzle isentropic efficiency (η_p), secondary nozzle isentropic efficiency (η_s) and diffuser isentropic efficiency (η_d) are taken to be 0.9. The cooling capacity (\dot{Q}_{evap}) of the refrigeration cycle is kept constant at 17 kW. The range of evaporator pressure is 240-490 kPa.

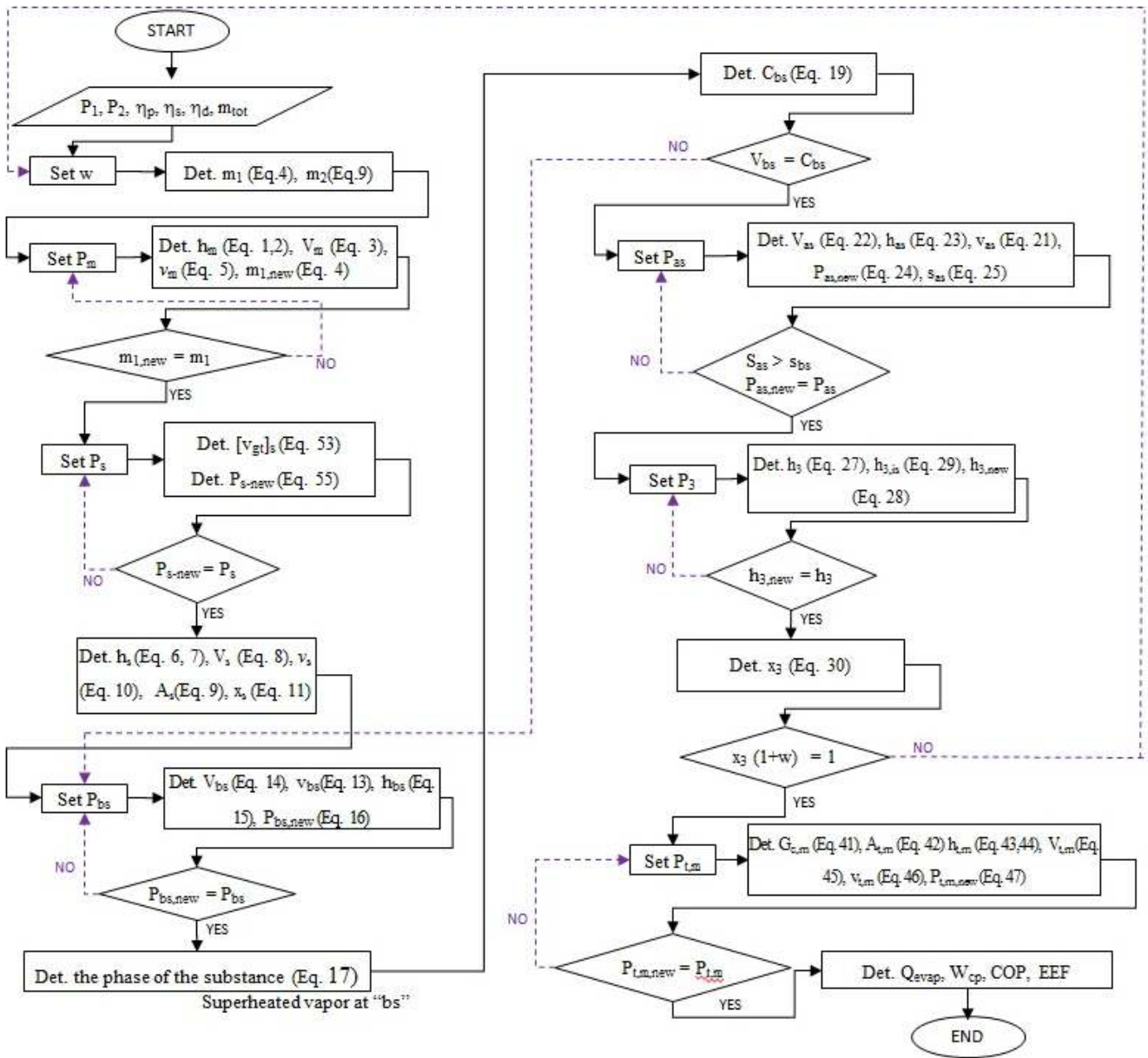


Figure 4. Flowchart of simulation program for EERC with constant area ejector (Det. = determine).

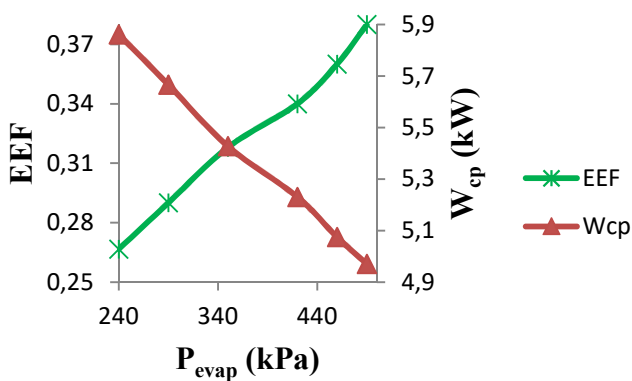


Figure 5. Variation of EEF and \dot{W}_{cp} with evaporator pressure (P_{evap}).

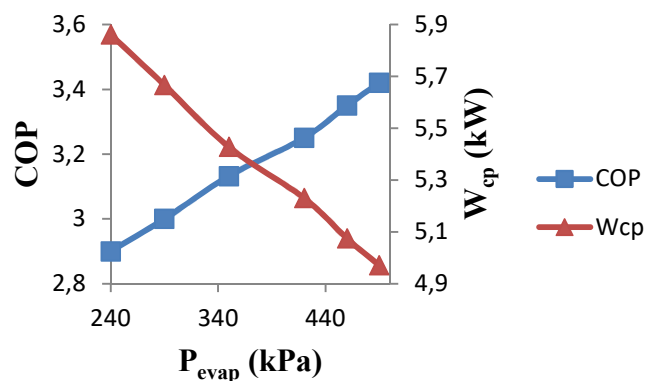


Figure 6. Variation of COP and \dot{W}_{cp} with evaporator pressure (P_{evap}).

As seen in Fig. 5, EEF of the ejector is increasing parallel with increase in P_{evap} . Since P_1 is constant, according to the definition of EEF (Eq. (68)), it is

inferred that ejector exit pressure (P_3) increases with increasing P_{evap} . This is attributed to the effect of increase in P_s at the secondary nozzle exit as P_{evap} increases. Increasing P_3 results in increasing P_6 (based on Eq. (61)) and h_6 . Since h_6 is equal to h_7 (Eq. (58)), cooling capacity (\dot{Q}_{evap}) gets lower with increasing P_3 , based on Eq. (59). In order to compensate this effect and to keep the \dot{Q}_{evap} constant, it is required to increase the secondary stream mass flow rate (m_2) as P_{evap} gets higher. In summary, as P_{evap} increases, increase in m_2 and P_3 values with accompanying increase of EEF is observed.

To express the above mentioned operational characteristics of the system, it could be remarked that the mass flow rate through nozzle is driven by the pressure difference through the nozzle. As P_{evap} increases at constant condenser pressure (P_{cond}), secondary nozzle back pressure (P_s) increases but rate of increase is lower than that of P_{evap} . Due to higher pressure difference across the nozzle ($P_2 - P_s$), secondary stream mass flow rate (m_2) increases with increasing P_{evap} . Therefore, for constant m_{tot} , the motive stream mass flow rate (m_1) reduces with increasing P_{evap} .

In Fig. 6, variation of COP and compressor power consumption (\dot{W}_{cp}) with increasing P_{evap} is shown. It is seen that response of COP to increasing P_{evap} is similar to that of EEF, i.e., COP increases with increasing P_{evap} . Based on Eq. (67), COP is directly associated with \dot{W}_{cp} . Due to the aforementioned system characteristics of: decreasing motive stream mass flow rate (m_1 , mass flow rate of the refrigerant which enters into the compressor) and increasing ejector exit pressure ($P_4 = P_3$, compressor inlet pressure) as P_{evap} increases, it is expected to see decreasing \dot{W}_{cp} as seen in Fig. 5 and Fig. 6.

In conclusion, for the case of constant \dot{Q}_{evap} , increasing P_{evap} results in EEF and COP increase and \dot{W}_{cp} reduction for considered EERC.

4.2. Effect of Condenser Pressure

In Fig. 7, COP and compressor power consumption of the refrigeration cycle (\dot{W}_{cp}) with respect to variation of condenser pressure (P_{cond}) is

seen for constant evaporator pressure of 415 kPa.

Additionally, variation of EEF and \dot{W}_{cp} of the refrigeration cycle with evaporator pressure (P_{evap}) is reported in Fig. 8. In the analysis, primary nozzle isentropic efficiency (η_p), secondary nozzle isentropic efficiency (η_s) and diffuser isentropic efficiency (η_d) are taken to be 0.9. The cooling capacity (\dot{Q}_{evap}) of the refrigeration cycle is kept constant at 17 kW. The range of condenser pressure is 1.3 - 2.1 MPa.

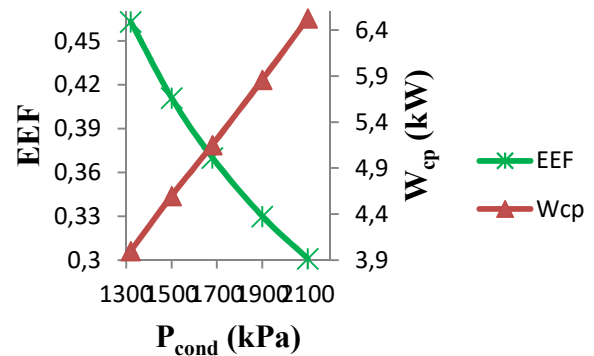


Figure 7. Variation of EEF and \dot{W}_{cp} with condenser pressure (P_{cond}).

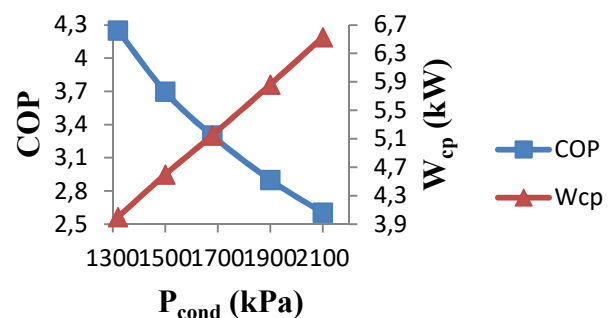


Figure 8. Variation of COP and \dot{W}_{cp} with condenser pressure (P_{cond}).

In Fig. 7, reduction of EEF with increasing condenser pressure (P_{cond}) is seen. As P_{cond} increases at constant evaporator pressure, primary nozzle back pressure (P_m) increases. Increase in P_m causes increase in resulting P_3 pressures. But the rate of increase in P_m and P_3 is lower than that of P_{cond} . As a result, EEF values gets lower as P_{cond} increases based on Eq. (68). Another result is: pressure difference of ($P_1 - P_m$) increases as P_{cond} gets higher. Since the mass flow rate through nozzle is driven by the pressure difference ($P_1 - P_m$), motive stream mass flow rate (m_1) increases with increasing P_{cond} .

The reasons of cooling capacity (\dot{Q}_{evap}) decrease with increasing P_3 are stated above. In order to keep the \dot{Q}_{evap} constant, it is required to increase also the secondary stream mass flow rate (m_2).

It is seen from Fig. 7 and Fig. 8 that compressor power consumption (\dot{W}_{cp}) increases with increase in P_{cond} . As it is mentioned above, reduction of \dot{W}_{cp} can be performed by two concurring factors: increase in P_3 and decrease in m_1 . But, despite the presence of increasing P_3 values, increase of m_1 is the prevailing factor on \dot{W}_{cp} . As a result, \dot{W}_{cp} increases with increasing P_{cond} as seen in Fig. 7 and Fig. 8, i.e., COP decreases with increasing P_{cond} based on Eq. (67).

4.3. Effect of Cooling Capacity

Effect of variation in cooling capacity of EERC (\dot{Q}_{evap}) to COP and EEF is seen in Fig. 9 when evaporator pressure (P_{evap}) is 415 kPa, condenser pressure (P_{cond}) is 1.8 MPa, primary nozzle isentropic efficiency (η_p), secondary nozzle isentropic efficiency (η_s) and diffuser isentropic efficiency (η_d) are taken to be 0.9. Cooling capacity of the EERC changes from 10 to 100 kW.

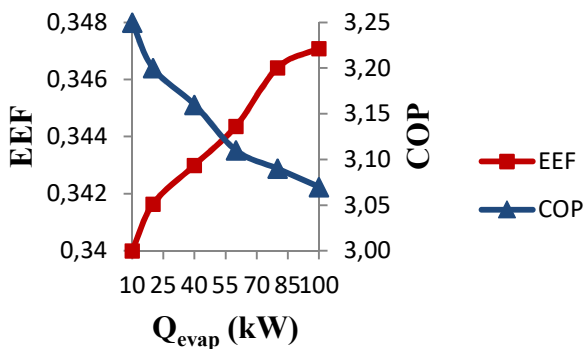


Figure 9. Variation of EEF and COP with \dot{Q}_{evap} .

As seen in Fig. 9, effect of increasing \dot{Q}_{evap} on COP and EEF is quite limited. The main reason is: to supply increasing rate of cooling performance (\dot{Q}_{evap}), variation of P_3 values is negligible due to the necessary modifications in main diameters of the ejector. Presenting the effect of considered operational parameters on design conditions of the ejector would cause an overcrowding of information, results and tables in this single study

which is avoided here. But, it is determined that P_3 is mainly a function of operational conditions and they are constant in this case. As a result, since change of P_3 values are limited, EERC system response to increasing \dot{Q}_{evap} in terms of EEF is very limited (Fig. 9).

A very slight decrease of COP can be observed in Fig. 9 as \dot{Q}_{evap} increases. In order to perform higher \dot{Q}_{evap} under fixed operational conditions, it is necessary to increase the refrigerant mass flow rate passing through the evaporator which is m_2 . To balance the system, simultaneous increase occurs in m_1 values, i.e., mass flow rate of the refrigerant at the input of the compressor gets higher. As a result, higher compressor power consumptions are seen as \dot{Q}_{evap} increases. In other words, as stated above, increase of m_1 affects \dot{W}_{cp} in increasing direction. Thereby, based on Eq. (67), COP values are balanced and variation of COP is quite limited as presented in Fig. 9.

5. CONCLUSION

In this present study, a 1-D analysis of EERC system with a constant area ejector which operates at critical mode is performed. In order to perform the analysis, a simulation program is developed using EES software and the effects of variation in evaporator pressure (P_{evap}) and condenser pressure (P_{cond}) and cooling capacity (\dot{Q}_{evap}) to ejector expansion factor (EEF) and coefficient of performance (COP) are investigated. Based on the above reported results, the following conclusions are drawn:

As the evaporation pressure (P_{evap}) of the EERC increases from 240 kPa to 490 kPa:

- EEF values rise from 0.26 to 0.38 (increased by 42%)
- COP values rise from 2.9 to 3.42 (increased by 18%)

As the condenser pressure (P_{cond}) of the EERC increases from 1.3 MPa to 2.1 MPa:

- EEF values reduce from 0.46 to 0.3 (decreased by 35%)
- COP values reduce from 4.25 to 2.6 (decreased by 38%)

As the cooling capacity (\dot{Q}_{evap}) of the EERC increases from 10 to 100 kW:

- EEF values rise from 0.34 to 0.347 (increased by 2%)

- COP values reduce from 3.25 to 3.07 (increased by 5%)

It can be concluded from above listed results that variation of P_{evap} and P_{cond} have adverse effects on EEF and COP. It is also determined that, due to the necessary modifications in main diameters of the ejector, variation of \dot{Q}_{evap} affects EEF and COP values quite slightly.

Nomenclature

A	Cross-sectional area (m ²)
COP	Coefficient of performance
h	Specific enthalpy (kJ/kg)
Ma	Mach number
P	Pressure (kPa)
s	Specific entropy (kJ/kg K)
T	Temperature (°C)
V	Velocity (m/s)
v	Specific volume (m ³ /kg)
w	Entrainment ratio
x	Quality
Q	Heat transfer rate (kW)
W	Power (kW)
η	Isentropic efficiency
1,2,3...,7	Number of points in Fig. 2
Subscripts	
cond	Condenser
evap	Evaporator
is	Isentropic
m	Primary nozzle
s	Secondary nozzle
t	Throat
tot	Total

REFERENCES

- [1] J. Sarkar, "Geometric parameter optimization of ejector expansion refrigeration cycle with natural refrigerants," *Int. J. Energy Res.*, vol. 34, pp. 84-94, 2010.
- [2] N. Lawrence and S. Elbel, "Experimental and analytical investigation of automotive ejector air conditioning cycles using low-pressure refrigerants," in *Proceedings of Int. Air Conditioning and Refrigeration Conference*, Purdue, West Lafayette, USA, 2012.
- [3] S. Gurulingam, A. Kalaiselvane and N. Alagumurthy, "Performance Improvement of Forced Draught Jet Ejector Using Constant Rate Momentum Change Method," *International Journal of Engineering and Advanced Technology*, vol. 2, pp. 149-153, 2012.
- [4] D. Li, "Investigation of An Ejector-Expansion Device in A Transcritical Carbon Dioxide Cycle For Military Ecu Applications," West Lafayette, Indiana, USA, 2006.
- [5] B. J. Huang, J. M. Chang, C. P. Wang and V. A. Petrenko, "A 1-D analysis of ejector performance," *Int. J. Refrig.*, vol. 22, pp. 354-364, 1999.
- [6] W. Chen, M. Liu, D. Chong, J. Yan, A. B. Little and Y. Bartosiewicz, "A 1D model to predict ejector performance at critical and sub-critical operational regimes," *International Journal of Refrigeration*, vol. 36, pp. 1750-1761, 2013.
- [7] L. Boumara and L. André, "Modeling of an ejector refrigerating system operating in dimensioning and off-dimensioning conditions with the working fluids R142b and R600a," *Applied Thermal Engineering*, vol. 29, p. 265-274, 2009.
- [8] B. J. Huang and J. M. Chang, "Empirical correlation for ejector design," *International Journal of Refrigeration*, vol. 22, p. 379-388, 1999.
- [9] J. T. Munday and D. F. Bagster, "A new ejector theory applied to steam jet refrigeration," *Ind. Engng Chem. Process Des. Dev.*, vol. 16, p. 442-449, 1977.
- [10] I. W. Eames, S. Aphornratana and H. Haider, "A theoretical and experimental study of a small-scale steam jet refrigerator," *International Journal of Refrigeration*, vol. 18, p. 378-386, 1995.
- [11] N. H. Gay, "Refrigerating System". US Patent 1,836,318, 1931.
- [12] C. A. Kemper, G. F. Harper and G. A. Brown, "Multiple-phase ejector refrigeration system". US Patent 3,277,660, 1966.
- [13] A. B. Newton, "Capacity control for multiple-phase ejector refrigeration systems". U.S. Patent 3,670,519, 1972.
- [14] A. B. Newton, "Control for multiple-phase ejector refrigeration systems". U.S. Patent 3,701,264, 1972.

- [15] A. A. Kornhauser, "The use of an ejector as a refrigerant expander," in *Proc. of the 1990 USNC/IIR-Purdue Refrigeration Conference*, West Lafayette, USA, 1990.
- [16] P. A. Domanski, "Theoretical Evaluation of the Vapor Compression Cycle With a Liquid-Line/ Suction-Line Heat Exchanger, Economizer, and Ejector," 1995. [Online]. Available: <http://citeseerx.ist.psu.edu/viewdoc/download?doi=10.1.1.600.603&rep=rep1&type=pdf>.
- [17] E. Nehdi, L. Kairouani and M. Bouzaina, "Performance analysis of the vapour compression cycle using ejector as expander," *International Journal of Energy Research*, vol. 31, pp. 364-375, 2007.
- [18] G. S. Harrell and A. A. Kornhauser, "Performance tests of a two phase ejector," in *Proc. of 30th Intersociety Energy Conversion Engineering Conference*, Orlando, FL, U.S.A., 1995.
- [19] M. Nakagawa, T. Matumi, H. Takeuchi and N. Kokubo, "Mixing of the confined jet of mist flow," *JSME International Journal - Series B*, vol. 39, pp. 381-386, 1996.
- [20] M. Nakagawa and H. Takeuchi, "Performance of two-phase ejector in refrigeration cycle," in *Proc. of the 3rd International Conference on Multiphase Flow*, Lyon, France, 1998.
- [21] S. Disawas and S. Wongwises, "M. Nakagawa and H. Takeuchi, "Performance of two-phase ejector in refrigeration cycle", in Proc. of the 3rd International Conference on Multiphase Flow, Lyon, France, 1998.," *International Journal of Refrigeration*, vol. 27, p. 587-594, 2004.
- [22] S. Wongwises and S. Disawas, "Performance of the two-phase ejector expansion refrigeration cycle," *International Journal of Heat and Mass Transfer*, vol. 48, pp. 4282-4286, 2005.
- [23] P. Chaiwongsa and S. Wongwises, "Effect of throat diameters of the ejector on the performance of the refrigeration cycle using a two-phase ejector as an expansion device," *International Journal of Refrigeration*, vol. 30, pp. 601-608, 2007.
- [24] P. Chaiwongsa and S. Wongwises, "Experimental study on R-134a refrigeration system using a two-phase ejector as an expansion device," *Applied Thermal Engineering*, vol. 28, pp. 467-477, 2008.
- [25] A. Khalil, M. Fatouh and E. Elgendy, "Ejector design and theoretical study of R134a ejector refrigeration cycle," *International Journal of Refrigeration*, vol. 34, pp. 1684-1698, 2011.
- [26] C. Seckin, "Effect Of The Primary Nozzle Throat Diameter on The Cooling Performance of An Ejector Expansion Refrigeration Cycle with A Two Phase Ejector Under Critical Conditions," in *Proc. of Istanbul International Conference On Progress In Applied Science*, Istanbul, Turkey, 2017.
- [27] B. Tashtoush, A. Alshare and S. Al-Rifai, "Performance study of ejector cooling cycle at critical mode under superheated primary flow," *Energy Convers. Manage.*, vol. 94, p. 300-310, 2015.
- [28] H. K. Ersoy and N. B. Sag, "Preliminary experimental results on the R134a refrigeration system using a two-phase ejector as an expander," *International Journal of Refrigeration*, vol. 43, pp. 97-110, 2014.
- [29] N. B. Sag, H. K. Ersoy, A. Hepbasli and H. S. Halkaci, "Energetic and exergetic comparison of basic and ejector expander refrigeration systems operating under the same external conditions and cooling capacities," *Energy Convers. Manage.*, vol. 90, p. 184-194, 2015.
- [30] R. Yapici, H. K. Ersoy, A. Aktoprakoglu, H. S. Halkaci and O. Yigit, "Experimental determination of the optimum performance of ejector refrigeration system depending on Ejector Area Ratio," *International Journal of Refrigeration*, vol. 31, p. 1183-1189, 2008.
- [31] E. D. Rogdakis and G. K. Alexis, "Investigation of ejector design at optimum operating condition," *Energy Conver Mngmnt*, vol. 41, p. 1841-1849, 2000.
- [32] M. Sokolov and D. Hershgal, "Enhanced ejector refrigeration cycles powered by low grade heat. Part 2. Design procedures," *International Journal of Refrigeration*, vol. 13, p. 357-363, 1990.
- [33] H. K. Abdel-Aal, A. S. Al-Zakri, M. El-Sarha and M. E. El-Swify, "Other options of mass and energy input for steam jet refrigeration systems," *ChemEngng J*, vol. 45, p. 99-110, 1990.
- [34] A. Selvaraju and A. Mani, "Analysis of an ejector with environment friendly

- refrigerants," *Appl. Therm. Eng.*, vol. 24, pp. 827-838, 2004.
- [35] J. Chen, H. Havtun and B. Palm, "Parametric analysis of ejector working characteristics in the refrigeration system," *Appl. Therm. Eng.*, vol. 69, pp. 130-142, 2014.
- [36] K. Sumeru, H. Nasution and F. N. Ani, "A review on two-phase ejector as an expansion device in vapor compression refrigeration cycle," *Renewable and Sustainable Energy Reviews*, vol. 16, p. 4927-4937, 2012.
- [37] K. Chunnanond and S. Aphornratana, "Ejectors: applications in refrigeration technology," *Renewable and Sustainable Energy Reviews*, vol. 8, p. 129-155, 2004.
- [38] M. Ouzzane and Z. Aidoun, "Model development and numerical procedure for detailed ejector analysis and design," *Appl. Therm. Eng.*, vol. 23, p. 2337-2351, 2003.
- [39] F. Liu and E. A. Groll, "Analysis of a Two Phase Flow Ejector For Transcritical CO₂ Cycle," in *Proc. of International Refrigeration and Air Conditioning Conference*, Purdue, USA, 2008.
- [40] R. E. Henry and H. K. Fauske, "The two-phase critical flow of one component mixtures in nozzles, orifices, and short tubes," *Journal of Heat Transfer*, vol. 93, pp. 179-187, 1971.
- [41] K. H. Ersoy, "Theoretical Investigation of Performance Characteristics of Ejector Refrigeration Systems (in Turkish)," Konya, Turkey, 1999.
- [42] Y. A. Cengel and M. A. Boles, *Thermodynamics: An engineering approach*, Boston: McGraw-Hill, 2001.
- [43] M. Hassanain, E. Elgendy and M. Fatouh, "Ejector expansion refrigeration system: Ejector design and performance evaluation," *International Journal Journal of Refrigeration*, vol. 58, pp. 1-13, 2015.
- [44] S. Elbel, "Experimental And Analytical Investigation of A Two-Phase Ejector Used For Expansion Work Recovery In A Transcritical R744 Air-Conditioning System," Urbana, USA, 2007.
- [45] K. Ameer, Z. Aidoun and M. Ouzzane, "Expansion of subcooled refrigerant in two-phase ejectors with no flux induction," *Experimental Thermal and Fluid Science*, vol. 82, p. 424-432, 2017.
- [46] M. E. Ahammed, S. Bhattacharyya and M. Ramgopal, "Thermodynamic design and simulation of a CO₂ based transcritical vapour compression refrigeration system with an ejector," *International Journal of Refrigeration*, vol. 45, pp. 177-188, 2014.
- [47] R. F. Tangren, C. H. Dodge and H. S. Seifert, "Compressibility Effects in Two-Phase Flow," *Journal of Applied Physics*, vol. 20, p. 637-645, 1949.
- [48] O. Brunin, M. Feidt and B. Hivet, "Comparison of the working domains of some compression heat pumps and a compression-absorption heat pump," *International Journal Journal of Refrigeration*, vol. 20, p. 308-318, 1997.